Chalcogenide glass thin film resists for grayscale lithography

A. Kovalskiy[1], J. Cech[1], C. L. Tan[1], W. R. Heffner[2], E. Miller[2],
C. M. Waits[3], M. Dubey[3], W. Churaman[3], M. Vlcek[4], H. Jain[1,2]

[1]Center for Optical Technologies, Lehigh University, PA, USA
[2]International Materials Institute on New Functionality in Glass, Lehigh University, PA, USA
[3]U.S. Army Research Laboratory, Adelphi, MD, USA
[4] Faculty of Chemical Technology, University of Pardubice, Czech Republic

ABSTRACT

The advantages and applications of chalcogenide glass (ChG) thin film photoresists for grayscale lithography are demonstrated. It is shown that the ChG films can be used to make ultrathin (~600 nm), high-resolution grayscale patterns, which can find their application, for example, in IR optics. Unlike polymer photoresists, the IR transparent ChG patterns can be useful as such on the surface, or be used to transfer the etched pattern into silicon or other substrates. Even if the ChG is used as an etch mask for the silicon substrate, its greater hardness can achieve a greater transfer ratio than that obtained with organic photoresists. The suitability of ChG photoresists is demonstrated with inexpensive and reliable fabrication of ultrathin Fresnel lenses that are transparent in the visible as well as in the IR region. The optical functionality of the Fresnel lenses is confirmed. Application of silver photodissolution in grayscale lithography for MEMS applications is also shown. The process consists of the following steps: ChG film deposition, Ag film deposition, irradiation through a grayscale mask, removal of the excess Ag and the transfer of the pattern to Si by dry etching. A substrate to ChG thickness etching ratio of ~ 10 is obtained for the transfer of patterns into silicon, more than a five fold increase compared to traditional polymer photoresist.

Keywords: chalcogenide glass, photoresist, grayscale, lithography, Fresnel lenses, dry etching, wet etching

1. INTRODUCTION

Modern grayscale photo- and electron-beam lithography allows the creation of continuous multi-level surface relief micro- and nanostructures and is commonly used in microoptics, MEMS/NEMS and biomedical devices.[1-5] Most of the grayscale lithography processes are based on conventional planar lithography photoresists, typically polymers. Grayscale lithography using polymer photoresists has been successful for making large area gradient profiles with the aim of further transfer to a substrate, usually silicon, with deep reactive ion etching (DRIE). For example, phase Fresnel lenses developed on polymer photoresists with initial pattern height of 3 μm could be transferred into silicon with the appropriate phase shift at each point on the lens with a DRIE etch selectivity of 15:1.[6] Another promising advanced method for the development of relatively thin Fresnel lenses (~4 μm) was proposed using a binary optics technique.[7]

The transfer of patterns into silicon may not always be needed or even desirable, especially when the photoresist itself may work as an optical component (e.g. a refracting surface). A 3D optical element patterned through a grayscale mask on the right resist material may itself possess the required optical properties[2], thus simplifying the device structure and fabrication considerably. The direct application of the patterned resists could significantly reduce the cost and time of fabrication as well. Different types of glass resists (sol-gel[2], chalcogenide glasses (ChG)[8]), which are much harder than polymers, are often proposed for such applications. Also polymers are not always suitable for ultrathin and nanosize structures, when one needs a resist material that is highly sensitive to irradiation, easily structured on the nanoscale, and is hard enough to be applied straightforward or transferred into silicon substrate. In this paper, we propose ChG thin film photoresists as prospective materials to produce ultrathin (~ 600 nm) grayscale patterns. They are also expected to yield better control of the geometry than is possible with polymer resists. Our materials have an additional remarkable property of radiation induced diffusion of silver, which opens new opportunities for grayscale lithography. Light, X-ray

Advances in Resist Materials and Processing Technology XXVI, edited by Clifford L. Henderson,
Proc. of SPIE Vol. 7273, 72734A · © 2009 SPIE · CCC code: 0277-786X/09/$18 · doi: 10.1117/12.811646

or e-beam irradiation causes complete dissolution of thin (up to ~ 50 nm) silver layer deposited on top of a ChG film, gradually changing the chemical resistance of the latter depending on the time and intensity of irradiation and thickness of silver layer.[4,9]

2. PROPERTIES OF CHALCOGENIDE GLASS PHOTORESISTS

Thin films of ChG (alloys of S, Se, and Te with more positive elements) possess the unique ability to change their structure and, consequently, their chemical resistance under the influence of light (UV, visible radiation with an energy greater than or equal to the band gap of the ChG layer), X-rays and electrons. The films investigated in this work are prepared by conventional thermal evaporation in vacuum. Structurally, most of the ChG can be considered as rigid polymers having network-like structure but without large molecular units. For such thin film structure the smallest feature size for patterning is determined by the type of irradiation, not the resist itself. The finest features of ~7 nm size (fig. 1) have been fabricated in our laboratory by exposing $As_{35}S_{65}$ thin film to low energy electron beam followed by wet etching.[10] Fig. 2 clearly shows well resolved spots at the ten nanometer scale on an e-beam irradiated surface of As_2S_3 thin film.

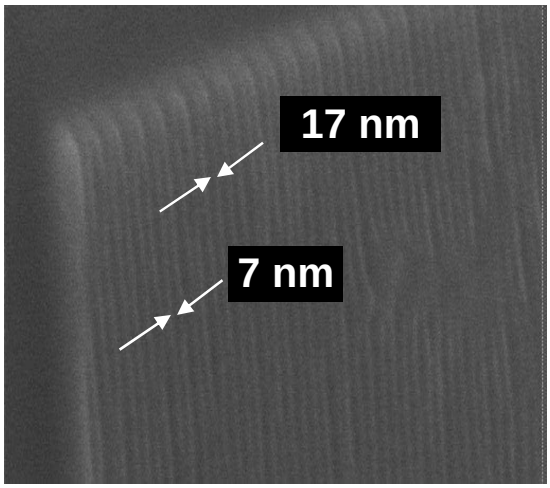

Fig. 1. SEM pictures of e-beam patterned and wet etched $As_{35}S_{65}$ ChG thin film: line separation ~ 7 nm, width ~17 nm and height ~ 80 nm – apparently the finest structure made in a glass.

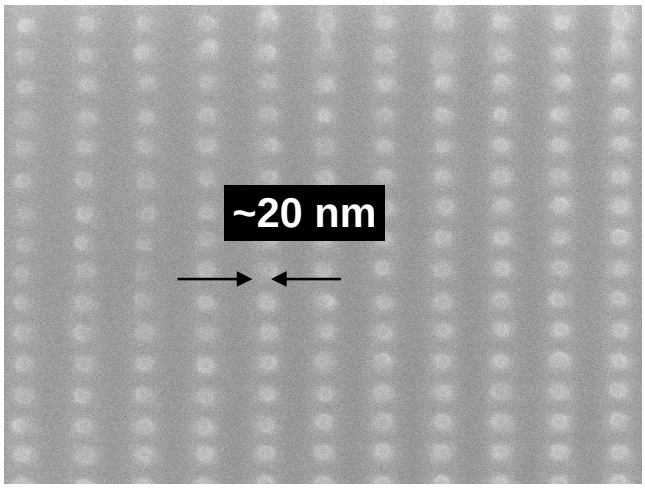

Fig. 2. Demonstration of the separate e-beam spots on the surface of wet etched electron irradiated As_2S_3 ChG thin film.

In addition to higher resolution, ChG thin films have several other advantages over polymers, such as higher hardness and higher resistance to acids. They are also suitable for selective etching of SiO_2, Si, Cr, etc., which are used in microelectronic processing. It is also important to note that the pre-baking and post-baking steps of polymer based lithography are completely eliminated. Moreover, by simply changing the composition of the wet developer, certain chalcogenide glass can be used both as a positive or a negative photoresist.[8]

An example of such dual behavior has been demonstrated on thin films of stoichiometric As_2S_3, which can serve as a positive or negative photoresist depending on the alkaline developer used.[11] The kinetics of As_2S_3 thin film dissolution (positive etching) in the aqueous solution Na_2CO_3 + Na_3PO_4 is presented in fig. 3. With non-aqueous, amine-based solvents an As-based ChG film usually behaves as a negative resist (fig. 4). The latter is mostly used for grayscale patterns like optical lenses.[12] Furthermore, ChG could also be negatively etched in plasma containing the gas mixtures of CF_4, Ar and O_2.[13]

The mechanism of selective etching follows from the structural features of as-prepared ChG thin films. Bulk stoichiometric ChG such as $As_2(S,Se)_3$ and $Ge(S,Se)_2$ consist of pyramidal $As(S,Se)_{3/2}$ or tetrahedral $Ge(S,Se)_{4/2}$ structural units, respectively. Homopolar bonds in such glasses are possible, in principle, only upon deviation from

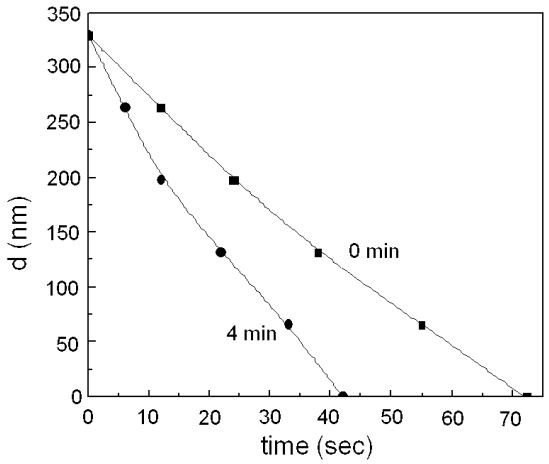

Fig. 3. Kinetics of dissolution of as-evaporated and 4 min exposed As_2S_3 film (d_0 = 330 nm) in aqueous solution of Na_2CO_3 + Na_3PO_4 (positive etching).

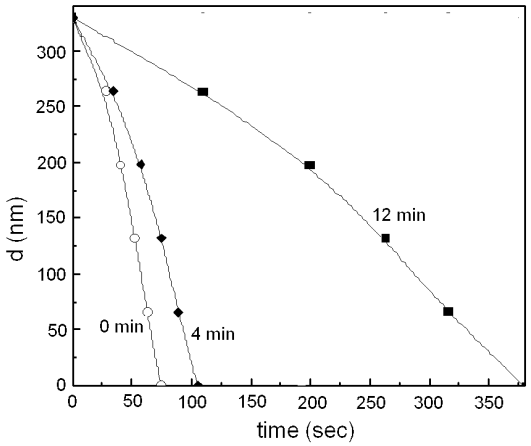

Fig. 4. Kinetics of dissolution of as-evaporated and different time exposed $As_{35}S_{65}$ film (d_0 = 330 nm) in non-aqueous amine based solution (negative etching).

stoichiometry. However, as-prepared ChG thin films, even of stoichiometric compositions, contain a considerable fraction of "wrong" (the bonds which should not exist in bulk glasses of stoichiometric compositions) homopolar bonds (As-As, S-S, Se-Se, Ge-Ge). Concentration of such "wrong" bonds in the structure of as evaporated films can vary from a few % to more than 10% depending on the conditions of thermal evaporation and can be consequently changed by exposure to radiation. Let us again demonstrate this difference in the structure of bulk, as evaporated and exposed films (which is responsible for selective etching) of the stoichiometric As_2S_3. In principle only AsS_3 pyramidal units should form the structure of stoichiometric As_2S_3 (each sulfur must be shared by two neighboring AsS_3 pyramids). Raman spectra of the bulk sample confirm validity of this concept – there the dominant broad band at 345 cm^{-1} corresponds to the presence of AsS_3 pyramids (fig. 5a). This band is slightly modified by shoulders at 312 and 380 cm^{-1} which are assigned to the interactions between these AsS_3 pyramids. In contrast, the Raman spectra of as evaporated film (fig. 5b) show very intense bands between 135 cm^{-1} and 234 cm^{-1} and also at 363 cm^{-1} which can be assigned to the vibration of As-As containing units[14], such as As_4S_4, together with additional relatively strong double band with maxima at 495 cm^{-1} and 474 cm^{-1}. These two bands are evidence that S-S containing structural units such as –S-S– chains are present and connect individual AsS_3 pyramids (495 cm^{-1}) and S_8 rings (474 cm^{-1}).[15,16] Appearance of these structural units containing homopolar bonds in the structure of as evaporated As_2S_3 thin films can be explained by the following thermal dissociation reaction during evaporation:[17]

$$(As_2S_3)_{liq} \xrightarrow{kT} (As_4S_4)_{vap} + (S_n)_{vap}\,, \qquad (1)$$

where non-stoichiometric As_4S_4 unit contains homopolar As-As bond. Due to fast condensation of vapors on the cold substrate (room temperature) these structural units are frozen in the structure of as evaporated films and they are responsible for photosensitivity of these films.[11]

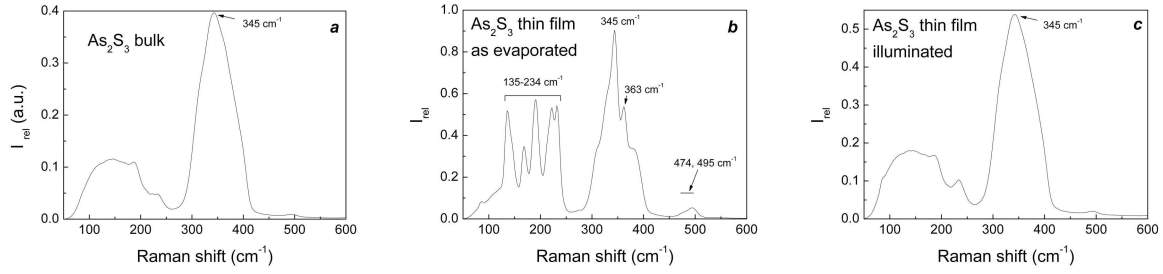

Fig. 5. Raman spectra of As_2S_3 samples: (a) bulk, (b) as evaporated thin film, (c) thin film after 30 minutes exposure with halogen lamp.

High-resolution X-ray photoelectron spectroscopy (XPS) is the perhaps the only method which gives us a fairly correct numerical value for the concentration of atoms in different chemical states. One can easily estimate the concentration of homopolar bonds from the areas of appropriate components of fitted XPS core level spectra. As an example, the XPS data for S 2p and As 3d core level spectra for an As_2S_3 thin film are presented in figs. 6 and 7. The areas I and II determine the concentration of atoms involved in heteropolar and homopolar bonds, respectively. The change in chemical resistance is a result in structural transformations caused by band-gap light or electron-irradiation of as-prepared films and is dependent on the type and intensity of irradiation, chemical composition and surface structure of the films. The relative concentration of the homopolar bonds is one of the key factors in the mechanism of these structural transformations.[11,17]

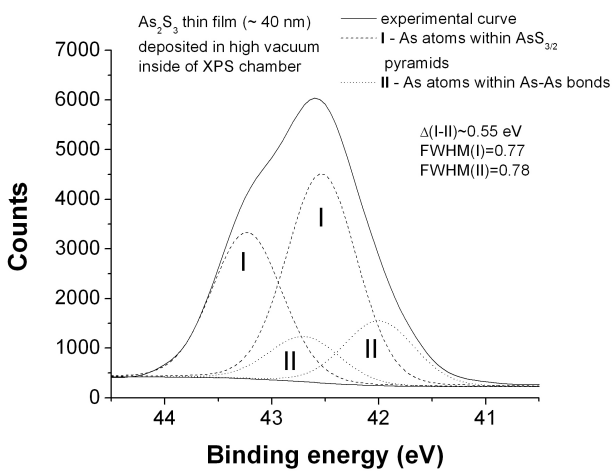

Fig. 6. Fitting of As 3d core level spectrum of as evaporated As_2S_3 thin film.

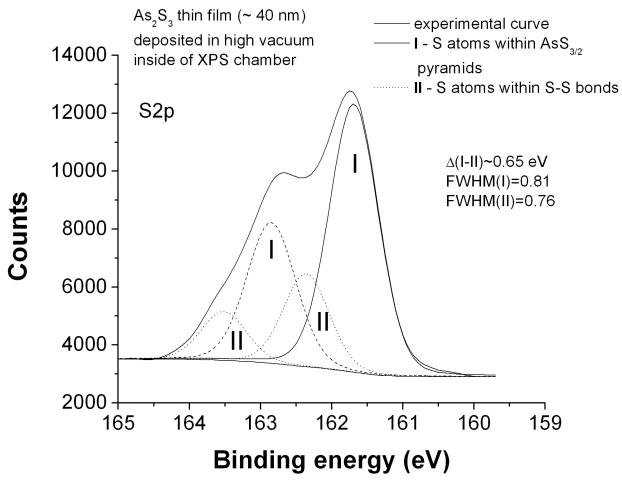

Fig. 7. Fitting of S 2p core level spectrum of as evaporated As_2S_3 thin film.

The mechanism of selective wet etching of As_2S_3 thin films (and other As based chalcogenides) in aqueous alkaline solutions is based on the different dissolution rates for AsS_3 pyramids, fragments with S-S homopolar bonds and As_4S_4 structural units with As-As homopolar bonds[18]. Concentration of homopolar bonds which is high in the structure of as evaporated films is reduced by exposure to radiation and the structure of the thin film becomes closer to the structure of bulk glass. Note the significant drop in the intensity of bands between 135 and 234 cm^{-1}, at 363 cm^{-1}, 474 cm^{-1} and 495 cm^{-1} in fig. 5c in comparison with fig. 5b after light illumination of the film due to the following polymerization reaction[8]:

$$As_4S_4 + S_n \xrightarrow{h\nu} As_2S_3, \tag{2}$$

leading to the change of chemical resistance.[11,19] The chemical reactions during etching of as evaporated and exposed films have different kinetics, thereby resulting in selective positive etching as described elsewhere.[18,20,21] Another probable chemical reaction influencing the selective etching efficiency is arsenic photo-oxidation on the surface of ChG thin film.[22]

Some authors[23,24] found negative selective etching of chalcogenide glass films in aqueous alkaline solvents. In this case, especially in chalcogen-rich compositions, the mechanism of dissolution is completely different due to the oxidation of As^{III+} arsenic to As^{V+} by polysulfide anions formed during the dissolution process in the etching bath and results in a negative type of etching, which is typical when amine based solvents are applied as described below. Negative resist behavior of As_2S_3 thin films in amine-based solvents can be described by the following reactions for the As_2S_3, As_4S_4 and S_n structural units:[17]

$$As_2S_3 + 6(C_2H_5)_2NH = [(C_2H_5)_2NH_2]_3AsS_3 + As[(C_2H_5)_2N]_3, \tag{3}$$

$$(C_2H_5)_2NH + S_n = (C_2H_5)_2NH^+S_n^-, \tag{4}$$

$$(C_2H_5)_2NH^+S_n^- + As_4S_4 \rightarrow (C_2H_5)_2NH_2^+S^-As_2S_2 + (C_2H_5)_2NAs_2S_2\,. \quad (5)$$

The negative character of the etching in amine-based solvents is explained by the faster rate of reactions (4) and (5) in comparison to reaction (3).[17]

Reactive ion etching (RIE) of ChG can be performed using different plasmas. The RIE method consists of two processes: spontaneous chemical reaction, which improves etching selectivity, and physical sputtering, which lowers selectivity between the materials. The first comprehensive study of RIE of As_2S_3 thin films showed that pure CF_4 plasma is highly isotropic causing unwanted undercutting of the film and too aggressive causing very rough sidewalls[13]. The isotropic behavior of CF_4 was greatly reduced using O_2 and Ar additives, with O_2/CF_4 having the best performance. Previous results of RIE of ChG show that good wall inclination angles (70° for CF_4/O_2 and 60° for CF_4 atmospheres, respectively) can be obtained.[25]

The Ge-based ChG film photoresists consist of more rigid tetrahedral molecular units of larger size, which may limit their application in grayscale and nanoscale photolithography. Strong Ge oxidation is another poorly regulated factor, which may adversely affect their lithographic applications. However, it was shown that these materials could be successfully utilized for ion-beam lithography.[26] Also they can be quite useful for the patterning based on controlled silver dissolution into ChG thin film, as described next.

The photo-induced silver dissolution can be used for fabricating three-dimensional (3D) grayscale masks in advanced micro-electromechanical systems (MEMS) and microelectronic technologies.[4,9] The smooth 3D microstructures in the ChG film can be transferred to Si by dry etching more accurately than with polymers used in traditional lithography owing to the higher hardness of the glass.

The mechanism of light-induced chemical interaction of Ag atoms with As_2S_3 matrix is based on the formation of Ag-S bonds on the surface of the film according to the following reactions:

$$(As-S)+Ag \xrightarrow{h\nu} (Ag-S)+As\,, \quad (6)$$

$$(S-S)+2Ag \xrightarrow{h\nu} 2(Ag-S)\,. \quad (7)$$

We purposely omit specifying the charge state of the atoms in reactions (6) and (7). It is the subject of a separate study. Reactions (6) and (7) are only one part of the mechanism of photodissolution, which is a much more complicated time/dose dependent process involving reversible changes, possible formation of an Ag-containing ternary, etc. A detailed explanation can be found elsewhere.[27] The confirmation of As separation at photodissolution is shown in fig. 8, where the removal of As atoms in HNO_3 solution is demonstrated by the XPS data. The As-removal process progresses linearly with time of irradiation from a halogen lamp.

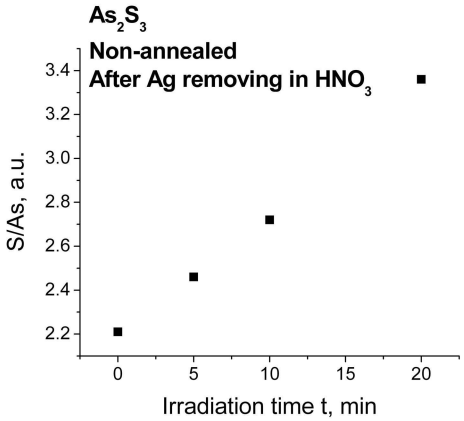

Fig. 8. Change of surface composition of the irradiated part of Ag/As_2S_3 sample with time of irradiation after development in dilute HNO_3.

3. ULTRATHIN FRESNEL LENSES ON CHALCOGENIDE GLASS As_2S_3 THIN FILMS

The sulfur-based chalcogenide glasses can be made transparent in a wide wavelength range from visible up to more than 12 μm using an optimized chemical composition. While irradiation of ChG by sub band gap light ($\lambda<\lambda g$, where λg is the wavelength corresponding to the band gap energy) may induce photostructural transformations accompanied by the change of optical properties, infrared light does not cause any photoinduced effects. That is why the most promising functionality of grayscale features on ChG resists has been microlens arrays for infrared applications.[8,9,12,28,29] For some applications in Si technology such as focal plane arrays for energy concentration or remote sensing an ultrathin (~600 nm) Fresnel lenses seems to be a very promising solution. They are capable of high

focus (small focal length) with wide aperture (diameter of Fresnel lens) within a thin layer of material. Successful attempts to obtain Fresnel lenses on ChG thin films have already been made.[30-32] However, either no optical characterization was reported or thickness of the lens layer was not particularly thin (>1.0 μm).

We selected the fabrication of a Fresnel lens and an array of similar lenses to demonstrate and establish the advantages of ChG as a material capable of forming complex optical structures in a single etching step. Aspheric (parabolic) height profile for the lens was calculated, assuming 2.35 as refractive index of ChG. The lens structure was designed for film thickness (i.e. maximum height of structure) of 600 nm, deposited on 475 μm thick silicon wafer, with the intention to focus 10 μm radiation from lens area to the backside of the wafer. Resulting height profile was assigned to 256 levels of gray, presuming linear dependency of gray level to final height transfer and all intermediate transfers. It was then converted to SVG (Scalable Vector Graphics) format using an especially developed program in the BASH scripting language. The SVG file was designed with 2048 individual ringlets for high precision. We reduced the resulting data file to a grayscale bitmap with 480×480 pixels, using bi-cubic re-sampling, and extracted pixels corresponding to 8 ranges of gray levels. The 8 bins/ranges for extraction were selected to be linear in the original 256 gray levels and extraction was performed by specially developed PYTHON program which can be used to process any bitmap to any number of bins. Output of this program was converted to filled rectangles as required using Nanometer Pattern Generation System (NPGS) electron lithography system (http://www.jcnabity.com), which uses DesignCAD LT 2000 as the plotting program. The method was selected due to inherent limitations of the most common lithographic data format, GDS-II, and due to the limitations of the NPGS system.

A HEBS (High Energy Beam Sensitive) blank glass mask was exposed to form the resulting NPGS pattern by electron beam, using LEO 1550 VT electron microscope, operating at 30 kV acceleration voltage, with 20 Pa of N_2 residual pressure to avoid charging. Each polygon was selected to cover the area of 980×980 nm to avoid accidental overlap. Polygons were composed by points, each having center-to-center distance and line distance of approximately 48 nm. Corresponding area dose was selected to be 0, 40, 80, 120, 160, 200, 240, 280 μC/cm^2 for each of the respective gray levels. The beam current was measured prior to and after writing, using a Faraday cup in the SEM microscope chamber. A number of grayscale masks with lens structures were inspected by optical microscope as shown in Fig. 9. There are no visible digital artifacts, although only 8 exposure levels (corresponding to 8 bins for original grayscale) and 480x480 rectangles were used. After inspection and cleaning in clean room, the mask was used for exposing the ChG film by contact lithography. The mask contained 2 types of Fresnel lens structures: individual lenses of 400 μm diameter (fig. 9) and arrays of lenses (480x480 μm^2) which consist of 16 lenses each.

To develop ultrathin Fresnel lenses on ChG, thin films of As_2S_3 were deposited onto glass and silicon substrates via high vacuum thermal evaporation-deposition. Optimum conditions for film formation on silicon wafers were established first by depositions on a test glass substrate. Next, the As_2S_3 film was exposed through the mask to 365 nm wavelength light of intensity 8.4 mW/cm^2 using a Karl SUSS MA-6 Mask Aligner in the clean room and then etched with a non-aqueous amine-based solvent. Suitable duration of irradiation and conditions of etching were established. Fresnel lenses were designed so that when etched into a chalcogenide film on a silicon substrate, the light would focus at a point on the back of the silicon wafer. The resulting lenses were examined under an optical microscope (fig. 10) and SEM (fig. 11) to determine whether the mask's grayscale integrity was maintained in the etched samples.

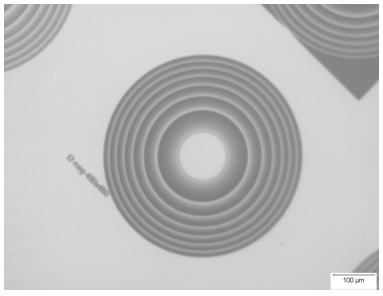

Fig. 9. Designed Fresnel lens mask on HEBS glass

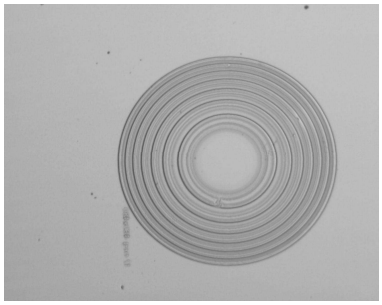

Fig. 10. Optical micrograph of Fresnel lens (thickness 600 nm) made of As_2S_3 film on silicon substrate.

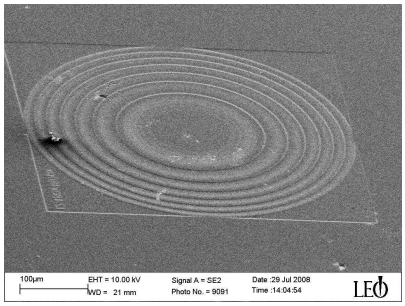

Fig. 11. SEM image of Fresnel lens made of As_2S_3 (thickness 600 nm) on silicon substrate

To determine whether the lenses had any optical functionality, the focal length of Fresnel lenses was measured using an optical microscope in transmission mode with the condenser removed. As the microscope objective is moved away from the top surface of the lensed substrate, the observed light cone decreases to a minimum radius above which it again increases. The position of minimum radius is taken as the focal point of the lens, and we report the focal length as the distance between the top surface of the lens and the position of minimum light cone radius. The pictures of the individual Fresnel lens of 400 μm diameter focused on the surface (a) and in the focal point (b) is shown in fig. 12. The focal length of the lenses is 5.38 mm and significantly differs from the calculated.

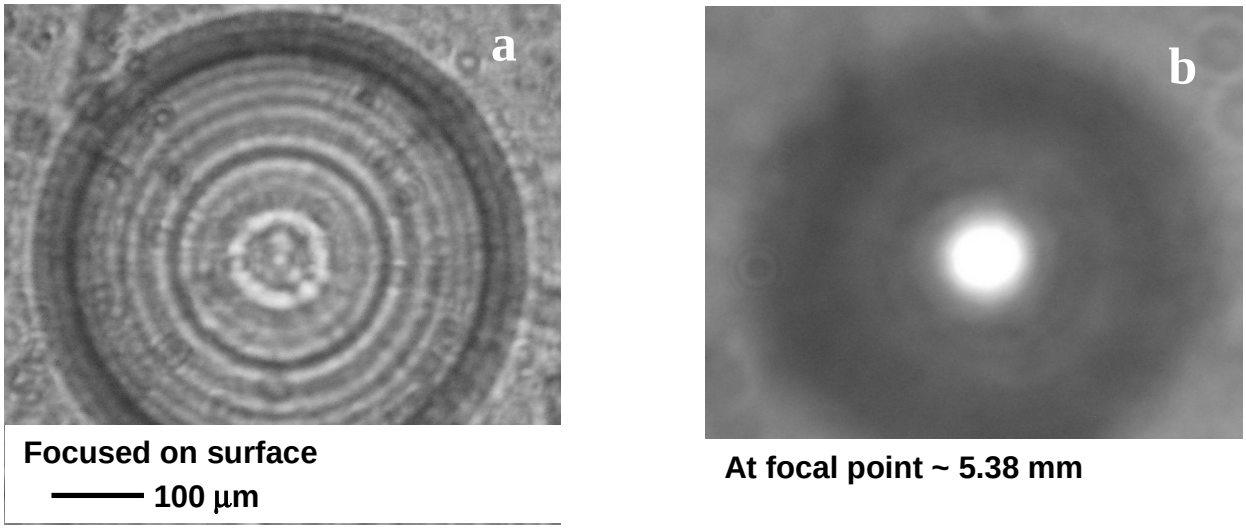

Fig. 12. Optical characterization of individual Fresnel lens (400 μm diameter, 600 nm thickness) on glass substrate: lens focused on the surface (a) and in the focal point (b)

The measurements of the focal length for the Fresnel lenses within the 480x480 μm^2 (fig. 13) arrays shows the magnitude ~300 μm, which is much closer to the calculated value.

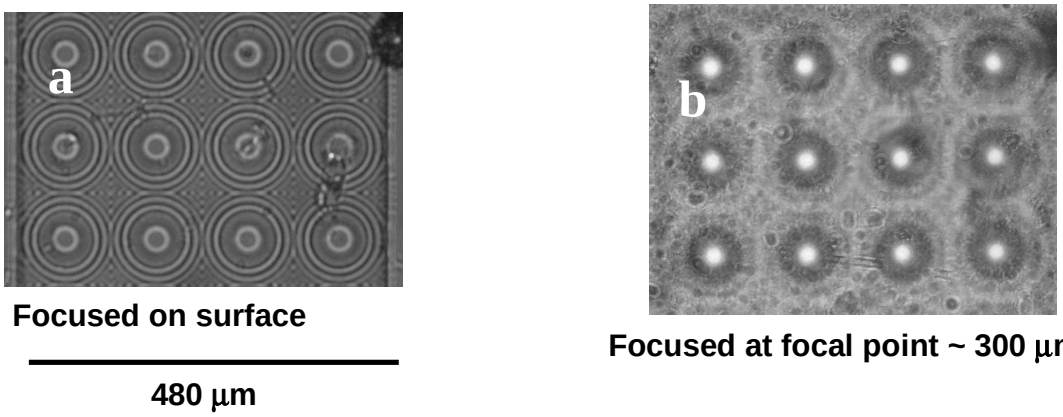

Fig. 13. Optical characterization of Fresnel lens array on glass substrate: lens focused on the surface (a) and in the focal point (b)

The lens deposited on the silicon substrate was characterized using a laser beam from an infrared laser (λ=1.55 μm) and charge-coupled device (CCD) camera. The light from the laser was directed on the unpolished side of the Si wafer, while the lens, which was developed on the opposite polished side, was placed facing the camera. As we can see from fig. 14a, the clear lens effect is observed confirming optical functionality of the Fresnel lens. For comparison, fig. 14b shows light through a flat As_2S_3 thin film, while fig. 14c presents a CCD image of the laser beam without the sample.

Fig. 14. CCD camera images of the beam focused by Fresnel lens on Si substrate (a), passing through plain ChG film on Si substrate (b) and direct laser beam (c). The scale bar in figure (a) is applicable to both figures (b) and (c).

4. GRAYSCALE LITHOGRAPHY BASED ON SILVER PHOTODISSOLUTION IN CHALCOGENIDE GLASS THIN FILMS

The dissolution of silver in ChG thin films under light, electron or X-ray (fig. 15) irradiation significantly changes its chemical resistance because of the gradual change of chemical composition. Grayscale lithography in ChG is based on the fact that both the exposure time, and light intensity affect the etching rate. Fig. 16 (right) shows the graph demonstrating change of etched depth with increasing of transparency of the grayscale features in the HEBS glass mask (left part of fig. 16, line A-A') uniformly exposed by halogen lamp light. The optical density through the mask ranged from 0.126 (shallowest etch of 65 nm) to 0.217 (deepest etch of 230 nm) allowing variation of the light intensity on glass surface. This dependence is close to linear demonstrating a uniform dissolution of silver to different depths that depend on the dose of irradiation (determined by its intensity and time of exposure). So a smooth shaping of more complex patterns from the grayscale optical mask is expected. The selectivity of the etching (defined as the etching rate ratio of exposed and unexposed material) is a function of thin layer composition, its prehistory as well as of etching gas composition. In our experiment, the etching depth was ~200 nm, although greater values are possible.

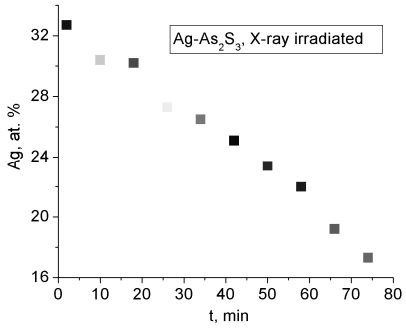

Fig. 15. Change of Ag concentration on the surface of As_2S_3 thin film with time of X-ray irradiation

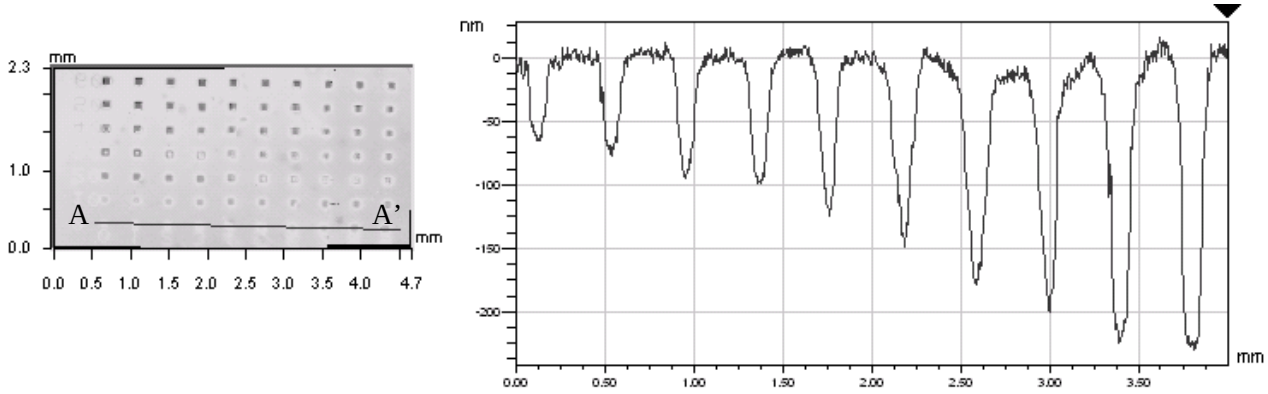

Fig. 16. Change of etching depth of Ag/As_2S_3 thin film layer with gradual variation of transparency of HEBS glass mask fragments.

Increased chemical resistance of ChG thin films after Ag dissolution offers opportunity to exploit dry RIE procedure for grayscale lithography. In this case, several additional variables influence the process, which include gas composition, gas

pressure (100–500 mTorr), flow rates (up to 100 sccm), substrate temperature (10-25 °C), electric power (70–200 W), and etch time. Other variables independent of etching method are film thickness, light intensity and exposure time.

For demonstrating grayscale patterning, the ChG thin film samples were irradiated with a halogen lamp (Fiber-Lite PL-Illuminator, Dolan–Jenner Industries) through a HEBS5 calibration plate containing grayscale features with gradual smooth change of transparency as well as lens-like structures. The time of exposure was varied widely from 1 to 200 min. After exposure, the residual undiffused silver was removed from unexposed parts using dilute HNO_3. Dry etching was carried out with a conventional system (Plasma Therm SSL-720) using CF_4 as the etchant gas. Pieces of the samples were mounted on unmasked 4-in Si wafer substrates using thermal grease (Cool-Grease TM 7016, AI Technology Inc.) in order to utilize the load lock on the RIE system. The variation of etch depth was measured and imaged using a VEECO NT1100 Optical Profiler.

Depending on the time of irradiation we were able to obtain negative or positive patterns. A section of complex grayscale structures, which was obtained by negative etching, is shown in fig. 17. In this case, the duration of irradiation by halogen lamp through grayscale mask was 2 min. The significant increase of irradiation time resulted in switching from negative to positive etching (fig. 18), probably due to the cascade of chemical reactions leading to the formation of Ag-enriched phase on the surface of the sample. The quality of the positive pattern is not as good as in the case of negative etching indicating that the uniformity of the surface is worse in the case of Ag-enriched composition. However, the observed switching from negative to positive etching simply by varying the irradiation time of Ag/As_2S_3 layer is a promising, new parameter for controlling grayscale patterning.

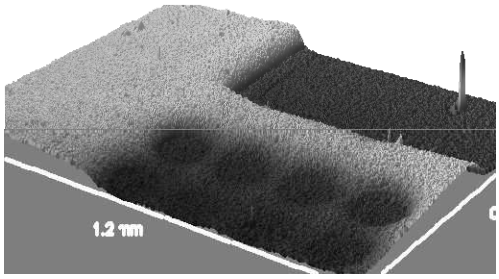

Fig. 17. Complex grayscale structure, obtained by negative RIE in CF_4 plasma

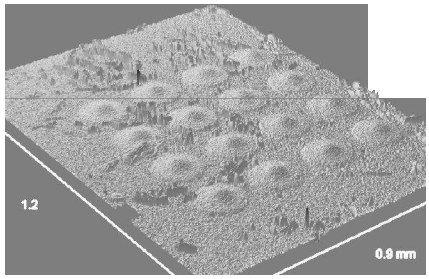

Fig. 18. Positive lens structure obtained after prolonged irradiation of Ag/As_2S_3 layer

Measurements of the etch depth of the positive features reveal that the average roughness of this pattern is ~ 50 nm (fig. 19). This value is unacceptably high for submicron lithography. In the case of our negative patterns presented in fig. 16, the average roughness usually is only a few nm and does not exceed the 20 nm level.

The exploratory experiments to transfer the grayscale patterns into Si substrate have given very encouraging results with an etch selectivity of 10:1 (Si etch rate: ChG etch rate), which should be significantly enhanced by the optimization of surface composition and RIE parameters, and decreased silicon loading by masking of the carrier wafer. This is a large increase over conventional polymer masking materials with an etch selectivity in RIE below 2:1. The higher etch selectivity of ChG films over traditional polymer films is associated with the increase in hardness, which reduces the amount of etching accomplished through physical sputtering from the energized ions in RIE.

CONCLUSIONS

Chalcogenide glass thin films are promising materials for use as high-resolution, grayscale photo- and electron-beam resists for nanoscale and ultrathin applications in MEMS/NEMS technology. They can be patterned directly to form IR transparent thin film lens array, Fresnel lenses, diffractive optical elements, etc. The fabricated ultrathin Fresnel lenses demonstrate desired optical functionality.

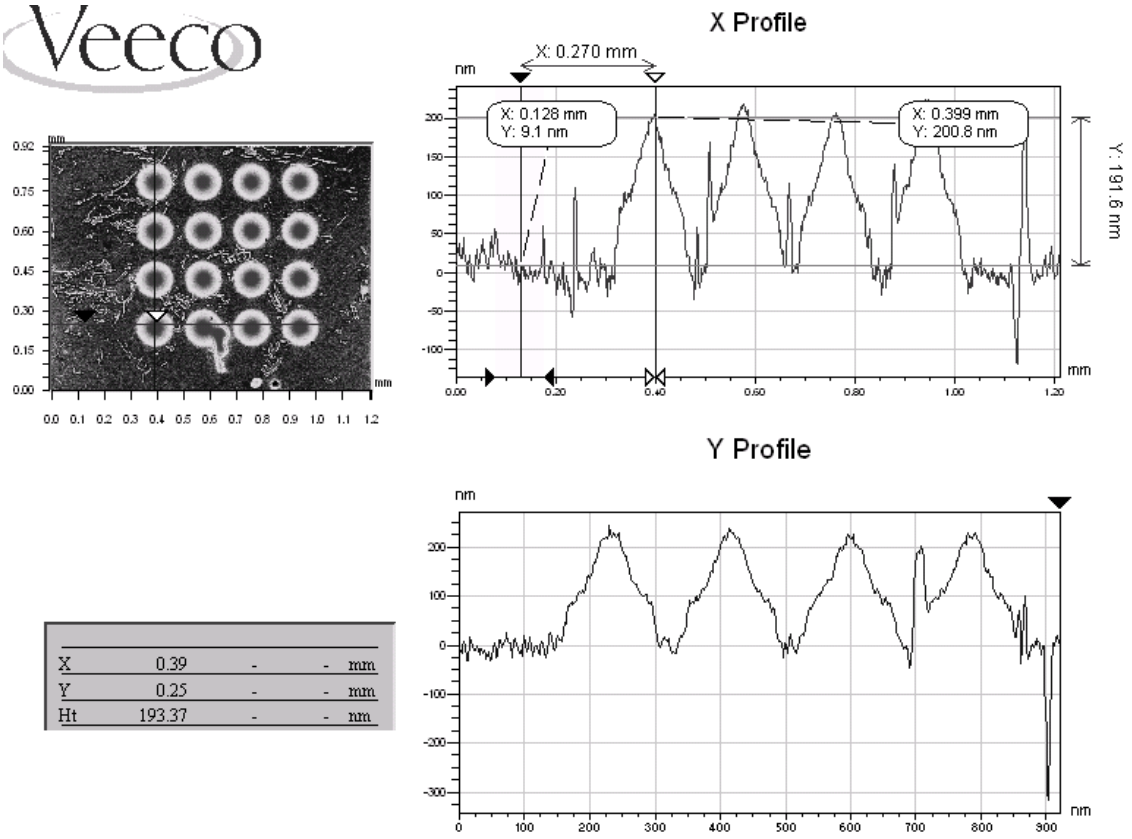

Fig. 19. Etch depth of the positively developed lens structures on Ag/As_2S_3 layers.

Photoinduced silver dissolution in ChG thin films introduces a new method for grayscale micropatterning. Nearly linear dependence of the etch depth on the total dose of absorbed light suggests that high-quality 3D patterning can be accomplished by dry reactive ion etching. Exploratory results show that the etch selectivity for transferring patterns into silicon is significantly superior to commonly used polymer resists used in lithography; process optimization should increase this ratio significantly. The technology will also be very useful in creating monolithically integrated memory devices using ChG on silicon substrates

Acknowledgement

Separate parts of this work were supported by Center for Optical Technology (Lehigh University), a Lehigh University—Army Research Lab (ARL) collaborative research program, the National Science Foundation (DMR 00-74624, DMR 03-12081, DMR 04-09588) and the Pennsylvania Department of Community and Economic Development through the Ben Franklin Technology Development Authority. M.V. thanks the Czech Ministry of Education, Youth and Sports for support under Grant 0021627501.

REFERENCES

[1] Kley, E.-B., "Continuous profile writing by electron- and optical lithography", Microelectron. Eng. 34, 261-298 (1997).
[2] Rogers, J. D., Kärkkäinen, A. H. O., Tkaczyk, T., Rantala, J. T. and Descour, M. R., "Realization of refractive microoptics through grayscale lithographic patterning of photosensitive hybrid glass", Opt. Express 12 (7), 1294-1303 (2004).

[3] Divliansky, I. B. and Johnson, E. G., "Three-dimensional diffractive micro- and nano-optical elements fabricated by electron-beam lithography", Proc. SPIE 6462, 64621B1-64621B8 (2007).
[4] Kovalskiy, A., Jain, H., Neilson, J. R., Vlcek, M., Waits, C. M., Churaman, W. and Dubey, M., "On the mechanism of grayscale patterning of Ag-containing As_2S_3 thin films", J. Phys. Chem. Solids 68, 920-925 (2007).
[5] Waits, C. M., Modafe, A. and Ghodssi, R., "Investigation of gray-scale technology for large area 3D silicon MEMS", J. Micromech. Microeng. 13 (2), 170-177 (2003).
[6] Morgan, B., Waits, C. M., Krizmanic J. and Ghodssi, R., "Development of a deep silicon phase Fresnel lens using gray-scale lithography and deep reactive ion etching", J. Microelelectromech. S. 13 (1), 113-120 (2004).
[7] Hanai, K., Nakahara, T., Shimizu, S. and Matsumoto, Y., "Fabrication of three-dimensional structures by image processing", Sensor. Mater. 18 (1), 49-61 (2005).
[8] Jain, H. and Vlcek, M., "Glasses for lithography", J. Non-Cryst. Solids 354, 1401–1406 (2008).
[9] Kovalskiy, A., Vlcek, M., Jain, H., Fiserova, A., Waits, C.M. and Dubey, M., "Development of chalcogenide glass photoresists for grayscale lithography", J. Non-Cryst. Solids 352, 589-594 (2006).
[10] Neilson, J.R., Kovalskiy, A., Vlcek, M., Jain, H. and Miller, F., "Fabrication of nano-gratings in arsenic sulphide films", J. Non-Cryst. Solids 353, 1427-1430 (2007).
[11] Vlcek, M., Prokop, J. and Frumar, M., "Positive and negative etching of As-S thin layers", Int. J. Electron. 77 (6), 969-973 (1994).
[12] Eisenberg, N.P., Manevich, M., Noach, S., Klebanov, M. and Lyubin, V., "New types of microlens arrays for the IR based on inorganic chalcogenide photoresists", Mat. Sci. Semicon. Proces. 3 (5-6), 443-448 (2000).
[13] Li, W., Ruan, Y., Luther-Davies, B., Rode, A. and Boswell, R., "Dry-etch of As_2S_3 thin films for optical waveguide fabrication", J. Vac. Sci. Technol. A 23 (6), 1626-1632 (2005).
[14] Shpotyuk, O.I., "Photostructural transformations in amorphous chalcogenide semiconductors", Phys. Stat. Sol. (b) 183 (2), 365-374 (1994).
[15] Kolobov, A.V., Kolomiets, B.T., Konstantinov, O.V. and Lyubin, V.M., "A model of photostructural changes in chalcogenide vitreous semiconductors. I. Theoretical considerations", J. Non-Cryst. Solids 45 (3), 335-341 (1981).
[16] Averyanov, V.L., Kolobov, A.V., Kolomiets, B.T. and Lyubin, V.M., "A model of photostructural changes in chalcogenide vitreous semiconductors. II. Experimental results", J. Non-Cryst. Solids 45 (3), 343-353 (1981).
[17] Zenkin, S.A., Mamedov, S.B., Mikhailov, M.D., Turkina, E.Yu. and Yusupov, I.Yu., "Mechanism for interaction of amine solutions with monolithic glasses and amorphous films in the As-S system", Glass Phys. Chem. 23 (5), 393-399 (1997).
[18] Vlcek, M., Frumar, M., Kubovy, M. and Nevsimalova, V., "The influence of the composition of the layers and of the inorganic solvents on photoinduced dissolution of As-S amorphous thin films", J. Non-Cryst- Solids 137&138, 1035-1038 (1991).
[19] Frumar, M., Cvrkal, M., Vlcek, M. and Wagner, T., "The photostructural changes and reactivity of chalcogenide layers", J. Non-Cryst. Solids 164-166 (2), 1243-1245 (1993).
[20] Hattori, M., Suzuki, H. and Enoki, Y., "Heats of solution of As-S, As-Se and As-S-Se glasses in alkaline solutions", J. Non-Cryst. Solids 52, 405-411 (1982).
[21] Bostick, B. C., Fendorf, S., Brown, G.E. Jr., "In situ analysis of thioarsenite complexes in neutral to alkaline arsenic sulphide solutions", Mineral. Mag. 69 (5), 781-795 (2005).
[22] Lucas, P., Wilhelm, A. A., Videa, M., Boussard-Pledel, C. and Bureau, B., "Chemical stability of chalcogenide infrared glass fibers", Corros. Sci. 50 (7), 2047-2052 (2008).
[23] Orava, J., Wagner, T., Krbal, M., Kohoutek, T., Vlcek, Mil. and Frumar, M., "Selective wet-etching of undoped and silver photodoped amorphous thin films of chalcogenide glasses in inorganic alkaline solutions", J. Non-Cryst. Solids 352, 1637-1640 (2006).
[24] Orava, J., Wagner, T., Krbal, M., Kohoutek, T., Vlcek, Mil. and Frumar, M., "Selective wet-etching and characterization of chalcogenide thin films in inorganic alkaline solvents" J. Non-Cryst. Solids 353, 1441-1445 (2007).
[25] Balan, V., Vigreux, C., Pradel, A., Llobera, A., Dominguez, C., Alonso, M. I. and Garriga, M., "Chalcogenide glass-based rib ARROW waveguide", J. Non-Cryst. Solids 326, 455-559 (2003).
[26] Lee, H.-Y. and Chung, H.-B., "Low-energy focused-ion-beam exposure characteristics of an amorphous $Se_{75}Ge_{25}$ resist", J. Vac. Sci. Technol. B 15 (4), 818-822 (1997).
[27] Jain, H., Kovalskiy, A. and Miller, A., "An XPS study of the early stages of silver photodiffusion in Ag/a-As_2S_3 films", J. Non-Cryst. Solids 352, 562-566 (2006).
[28] Saitoh, A., Gotoh, T. and Tanaka, K., "Chalcogenide-glass microlenses attached to optical-fiber end surfaces", Opt. Lett. 25 (24), 1759-1761 (2000).

[29] Smith, J. G. and Borek, G. T. “Etching of chalcogenide glass for IR microoptics”, Proc. SPIE 6940, 69400W (2008).
[30] Stronski, A. V., “Application of As-S-Se chalcogenide inorganic resists in diffractive optics”, Proc. SPIE 3729, 250-254 (1999).
[31] Eisenberg, N. P., Manevich, M., Arsh, A., Klebanov, M. and Lyubin, V., “New micro-optical devices for the IR based on three-component amorphous chalcogenide photoresists”, J. Non-Cryst. Solids 352, 1632-1636 (2006).
[32] Indutnyi, I. Z., Stronski, A. V., Kostioukevitch, S. A., Romanenko, P. F., Schepeljavi, P. E. and Robur, I. I., "Holographic optical element fabrication using chalcogenide layers", Opt. Eng. 34, 1030-1039 (1995).